

~~CONFIDENTIAL~~

Copy  
RM E54B18

NACA RM E54B18

**NACA**

# RESEARCH MEMORANDUM

EXPERIMENTAL SEA-LEVEL STATIC INVESTIGATION  
OF A SHORT AFTERBURNER

By James L. Harp, Jr., William E. Mallett  
and Thomas B. Shillito

Lewis Flight Propulsion Laboratory  
Cleveland, Ohio

**NOT REPRODUCIBLE**  
**NOT TO BE TAKEN FROM THIS ROOM**

CLASSIFICATION CHANGED

To UNCLASSIFIED

By authority of NASA memo Dated Mar. 12, 1963,  
s/p. m. Lovell  
for Boyd C. Myers II

CLASSIFIED DOCUMENT

This material contains information affecting the National Defense of the United States within the meaning of the espionage laws, Title 18, U.S.C., Secs. 793 and 794, the transmission or revelation of which in any manner to an unauthorized person is prohibited by law.

**NATIONAL ADVISORY COMMITTEE  
FOR AERONAUTICS**

**HR - 6-25-63**

**WASHINGTON**

May 11, 1954

~~CONFIDENTIAL~~



## NATIONAL ADVISORY COMMITTEE FOR AERONAUTICS

RESEARCH MEMORANDUM

## EXPERIMENTAL SEA-LEVEL STATIC INVESTIGATION OF A SHORT AFTERBURNER

By James L. Harp, Jr., William E. Mallett, and Thomas B. Shillito

## SUMMARY

A sea-level static investigation was conducted to determine the performance and some principles of design for a short afterburner. The power section of a 12-stage axial-flow turbojet engine was used in the investigation, and the afterburner was designed to fit within the length required for the tail pipe used on the standard nonafterburning model.

Development of a short afterburner configuration that was considered satisfactory for application was hampered by local hot spots on the outer shell of the afterburner and by screeching combustion. Both the outer-shell hot spots and the screeching combustion were eliminated by use of a perforated liner inside the outer shell, which extended from the flame holder to the exhaust nozzle. One short afterburner configuration incorporating this outer-shell liner gave an augmented thrust 1.33 times that of the standard nonafterburning model of the engine. This augmentation ratio of 1.33 does not represent the maximum augmentation available from the short afterburner but is the highest that could be obtained with the largest exhaust nozzle available at the time of the investigation. The nonafterburning thrust of this short afterburner configuration was 97 percent of the thrust of the standard nonafterburning model of the engine for the same operating conditions.

## INTRODUCTION

For take-off thrust augmentation of the engines of turbojet-powered bomber aircraft, afterburning is useful, particularly if it can be done without an increase of engine length or serious loss in the cruise specific fuel consumption. However, little is known about the performance and methods of design of short afterburners suitable for this application. A sea-level static investigation was therefore conducted at the NACA Lewis laboratory in order to provide information useful for the design of afterburners for take-off thrust augmentation.

The afterburner was shorter than is usually found in conventional designs and was arbitrarily designed to fit within the length required for the normal nonafterburning engine tail pipe. The short over-all length of the afterburner necessitated reducing the length of both the diffusing passage between the turbine outlet and the combustion zone of the afterburner to values below those customarily employed. Results of investigating a number of diffuser design modifications for the short afterburner are included in reference 1; these investigations were conducted without afterburning. The results obtained in the investigation of over-all performance with the afterburner in operation are presented herein.

The afterburner investigation was conducted at an engine-inlet temperature of 100° F and at an engine speed and turbine-discharge temperature near the military rated values for the engine. Investigation of a method of eliminating combustion screech (ref. 2) and afterburner-shell hot spots was concluded before a satisfactory configuration was obtained. Afterburner performance at two over-all engine-afterburner fuel-air ratios was obtained by using two fixed-area exhaust nozzles of different sizes. An indication of the loss in cruising specific fuel consumption was procured by running the engine without afterburning with an exhaust nozzle sized to give the preselected maximum turbine-discharge temperature.

## APPARATUS

### Engine and Installation

The engine used in the investigation was a production-model single-spool type with a 5-minute military sea-level static thrust rating of 5970 pounds at a rotor speed of 7950 rpm and an exhaust-gas temperature of 1275° F. The engine has a 12-stage axial-flow compressor, eight cylindrical combustion chambers, and a single-stage turbine.

The engine was mounted on a frame suspended from the ceiling of the test cell (fig. 1); and engine thrust, which was transmitted to the frame, was balanced and measured by a null-type air-pressure diaphragm. A diaphragm-type seal surrounded the engine tail pipe near the exhaust nozzle and isolated the main test cell from the exhaust sound-muffling chamber. The greater portion of the engine air was ducted from the atmosphere into the airtight test chamber through an air-measuring nozzle and ducting that discharged at the ceiling of the test cell. The remainder of the engine air was supplied by the laboratory high-pressure air system and entered the test chamber through a single can-type combustor that was used to maintain a fixed engine-inlet air temperature. Heating of the inlet air was accomplished by mixing the exhaust gas from the combustor with the atmospheric air ducted into the test chamber.

### Configuration Components

Over-all engine envelopes for both the standard nonafterburning engine and the engine equipped with the short afterburner are shown in figure 2. Both the standard tail pipe and the short afterburner were 54 inches long from the turbine-discharge flange to the exhaust-nozzle exit. Details of the various components used in the short afterburner configurations are included in the following sections.

Outer shells. - The outside contour of all outer shells used was the same. The basic outer shell was approximately 32 inches in diameter (fig. 2) and was equipped with a small quartz viewing window about 18 inches downstream of the turbine-discharge flange. One of the outer shells used in the investigation of combustion screech was equipped with longitudinal fins as shown in figure 3. These longitudinal fins consisted of strips of 0.125-inch-thick steel, 2 inches wide, mounted on the inside wall of the basic outer shell with the 2-inch dimension aligned radially (fig. 3(a)). The 25 longitudinal fins, spaced equally around the circumference, extended from 12 inches downstream of the turbine-discharge flange to the exhaust-nozzle inlet. Figure 3(b) is a photograph showing the portion of the longitudinal fins that was mounted in the straight section of the outer shell.

Another outer shell (fig. 4) was equipped with a cylindrical liner about 30.5 inches in diameter spaced inside the straight section of the basic outer shell. The liner, which was closed at the downstream end, was completely perforated with 0.188-inch-diameter holes on 0.5-inch centers. The annular space between the outer shell and the liner was left open at the upstream end.

Innerbodies. - The diffuser innerbodies used in the investigation are shown in figure 5. All innerbodies were surfaces of revolution. The modified curved innerbody was 18 inches long and 16 inches in diameter at the downstream end. The original curved innerbody, before modification, was 12 inches in diameter at the downstream end (ref. 1). The 18-inch straight innerbody was 18 inches long and 12 inches in diameter at the downstream end. Both the modified curved and the 18-inch straight innerbody were cupped at the downstream end. The over-all dimensions of the 18-inch slotted innerbody were the same as for the 18-inch straight innerbody, but the slotted innerbody differed in that its downstream end was not cupped and that it had a circumferential slot around the innerbody surface about 9 inches from the downstream face. The 24-inch innerbody was made up of two conical sections. The upstream conical section, which was 12 inches long, had the same included angle between the sides as the 18-inch straight innerbody and was 16.8 inches in diameter at the junction of the upstream and downstream sections. The downstream conical section was 12 inches long and 12 inches in diameter at the downstream end.

All innerbodies were equipped with vanes at the upstream end to straighten the whirl in the turbine-exhaust gases. A photograph of the straightening vanes on the innerbody, as well as those mounted on the outer shell, is shown in figure 5(b). Details of the design of these straightening vanes are given in reference 1.

Flame holders. - Flame holders used in the investigation are shown in figure 6. All these flame holders were composed of V-gutter sections with the primary elements arranged in annular rings. Single-ring flame holders with gutter widths of 0.75, 1.5, and 3.0 inches, and a two-ring flame holder with 0.75-inch gutters were used in the investigation. Each flame holder was equipped with four equally spaced radial elements that interconnected the annular rings with the blunt end of the innerbody. (For the flame holders used with the 24-inch innerbody, these radial gutter elements were removed.)

The single-ring 3-inch-gutter flame holder was modified for one phase of the investigation by the addition of a double-walled cylindrical splitter extending 16 inches downstream of the inside apex of the gutter. Water was circulated between the walls of the splitter to prevent damage during combustion. A photograph of the flame holder with the splitter plate installed is shown in figure 6(b).

Fuel-spray bars. - Sixteen spray bars equally spaced around the circumference of the afterburner were used for injection of fuel into the afterburner. The longitudinal location of the spray bars, which depended upon the particular configuration being investigated, is described in a subsequent section. The design criteria for the spray bars are illustrated in figure 7. The radial passage between the innerbody and the outer shell at the longitudinal station of interest was divided to give six equal annular areas. Two holes 0.030-inch in diameter were drilled in opposite sides of the spray bar to inject fuel normal to the air flow in the center of all except the outermost annular area increment.

Exhaust nozzles. - Three different exhaust-nozzle sizes were used in the investigation. One nozzle had an exit diameter slightly larger (20.5 in.) than required to give a tail-pipe temperature, without afterburning, of 1250° F at an engine speed of 7900 rpm and a compressor-inlet temperature of 100° F. Tabs at the nozzle exit were used to make the final adjustment of nozzle area to obtain the specified operating conditions for both the standard tail pipe and the short afterburner during nonafterburning operation. For afterburner operation, fixed exhaust nozzles with exit diameters of 24.25 and 25.50 inches were used. The effective flow area of each exhaust nozzle was reduced somewhat by the presence of instrumentation (subsequently described) in the plane of the exhaust-nozzle exit.

### Afterburner Configurations

The make-up of a typical short afterburner configuration is shown in figure 8. The flame holder for all configurations was located just downstream of station 7. The innerbody type, fuel-injection station, flame-holder type, outer-shell type, and exhaust-nozzle diameter used in the various configurations are summarized in table I.

### Instrumentation

Static pressures were measured on the wall of the test cell and in the exhaust sound-muffling chamber. The engine-inlet total pressure was not measured but was assumed to be equal to the cell static pressure. For nonafterburning runs of the afterburning configurations, total pressure was measured at station 7; measurements at seven different radial positions were made for the configuration with the 24-inch innerbody and at eight different radial positions for the other three innerbodies. Static pressure was measured on the outer-shell wall at station 7. Total pressure was measured by a water-cooled rake in the plane of the exhaust-nozzle exit for all configurations investigated. Details of the total-pressure measurements in the plane of the exhaust-nozzle exits are as follows:

Configuration	Number of measuring locations across nozzle diameter
Standard-engine tail pipe	14
Short afterburners:	
Nonafterburning	14
Afterburning	16

Temperatures were measured at the engine inlet, the turbine outlet, and, for nonafterburning runs, in the exhaust-nozzle-exit plane. Details of these temperature measurements are as follows:

	Rakes	Thermocouples in each rake	Total thermocouples	Rake location
Engine inlet	4	5	20	90° Apart at cowling entrance
Turbine outlet	6	5	30	5 In. downstream of turbine outlet
<sup>a</sup> Exhaust- nozzle inlet	1	14	14	Across nozzle exit

<sup>a</sup>Only for standard-engine tail-pipe and nonafterburning runs with short afterburner.

Air flow was measured by a 26-inch long-radius A.S.M.E. air-measuring nozzle in the main air-supply ducting (fig. 1) and by a flat-plate orifice in the preheater air-supply line. Fuel flow to the primary-engine combustors was measured by a rotameter and to the afterburner by a flat-plate orifice.

An electronic audio-oscillator was used in the determination of combustion-screach frequencies. The signal from the oscillator, which could be varied over the complete range of frequencies audible to the human ear, was used to energize a standard earphone. The audible tone that was associated with screeching combustion was matched by the output of the audio-oscillator, and the frequency was read directly from a calibrated scale.

#### PROCEDURE

The engine-inlet temperature was set at 100° F with the combustion heater for both afterburning and nonafterburning runs, so that a constant reference operating condition could be maintained. This temperature was selected as a practical minimum inlet temperature, since experience in operation at the test cell has shown that, on some warm days, temperatures below 100° F cannot be maintained at the engine inlet even without preheating.

Some nonafterburning runs were made to determine the performance of the engine at the preselected maximum values of engine speed and turbine-outlet temperature, 7900 rpm and 1250° F, respectively. A Strobotac was used to set engine speed for all runs, and 7900 rpm was the nearest speed

below the military rated value of 7950 rpm at which the intermittent light and the disk markings of the Strobotac were synchronized. A turbine-outlet temperature of 1250° F, instead of the military rated value of 1275° F, was used to prevent compromising engine life during any extended periods of operation at maximum engine speed and turbine-outlet temperature. The nonafterburning runs were made with both the standard tail pipe and afterburner configurations. The runs with the standard tail pipe provided a thrust value that served as a base for afterburning augmentation ratios. Nonafterburning runs with the afterburner configurations were made to evaluate diffuser performance and to determine the loss in engine cruise performance caused by the afterburner components.

The afterburner was started with the engine operating at maximum speed. Fuel to the afterburner was turned on and was then ignited by a hot streak from one of the primary-engine burners.

## DISCUSSION OF RESULTS

### Factors Controlling Development of Satisfactory Configuration

A short afterburner configuration that was considered satisfactory was evolved through consideration of the performance characteristics of a number of diffusers investigated in reference 1 and through correction of some undesirable afterburner operating characteristics that were manifest during the initial phases of the research program. These undesirable operating characteristics were outer-shell hot spots and screeching combustion. Performance characteristics of the diffusers are reviewed and experiences with the undesirable afterburner operating characteristics are reported herein for the benefit of future research on similar afterburners and as a guide to the design of units based upon similar considerations of short length.

Diffuser performance. - As discussed in reference 1, only a few of the diffuser innerbody configurations investigated showed promise for afterburner application. These configurations were, as designated in reference 1, the modified curved innerbody, the 18-inch straight innerbody, the 18-inch slotted innerbody, and the 24-inch innerbody, all of which were equipped with turbine-discharge whirl-straightening vanes. The factors considered in evaluating the diffusers for the short afterburner application were the over-all pressure loss in the diffuser and the tendency for flow to separate from the innerbody wall. An indication of over-all pressure losses is given in the following table, which shows the ratio of total pressure at the exhaust nozzle of the short afterburner configuration with the afterburner inoperative to the total

pressure at the exhaust nozzle of the standard nonafterburning engine under the same engine operating conditions, 7900 rpm and a tail-pipe temperature of 1250° F:

Configuration	Innerbody	Total-pressure ratio
1	Modified curved	0.976
2	18-Inch straight	.985
3	18-Inch slotted	.977
4	24-Inch with outer-shell liner	.967

The total-pressure loss from the turbine discharge to the exhaust-nozzle inlet for the standard nonafterburning engine is approximately 4 percent of the turbine-discharge pressure. As can be seen in the table, the total-pressure loss for the short afterburner configurations is from 1.5 to slightly over 3 percentage points greater than that for the standard nonafterburning tail pipe. The data shown in the table were obtained with a two-ring 0.75-inch-gutter flame holder installed in the afterburner. Similar data presented in reference 1, which were obtained without a flame holder, show that the pressure loss attributable to any of the four innerbodies used in configurations 1 to 4 was approximately 1 percentage point. The remaining loss of 0.5 to 2.0 percentage points is thus associated with the flame holder and outer-shell liner, and any improvements in over-all engine performance without afterburning would have to result largely from refinements of these components. A relatively free choice of afterburner configuration was permitted by the marginal differences in pressure loss among the configurations.

Another aspect of diffuser performance considered was the diffuser-outlet radial velocity profiles, which are shown in ratio form in figure 9 for configurations 1, 2, and 4. As pointed out in reference 1, velocity profiles for configuration 3 (slotted innerbody) were unreliable and are therefore not included in figure 9. The ratios of local velocity to peak velocity are for station 7 in the afterburner, the plane of the aft end of all but the 24-inch innerbody. Highest local velocities occurred toward the outer wall. Local velocities for all configurations were much lower near the inner wall, although no clear-cut cases of separation from the innerbody wall were evident for any of the four configurations.

The average bulk velocity at station 7, under the conditions of engine operation applicable to the data shown in figure 9, was from 540 to 625 feet per second for the configurations shown. A more uniform distribution of velocity than shown in figure 9 is desirable from consideration of factors involved in the combustion process, but numerous

changes in diffuser design reported in reference 1 did not yield significant improvement over the profiles shown. No one of the configurations shown in figure 9 was markedly superior; and, again, as in the consideration of pressure-loss characteristics, a relatively free choice of diffuser design for an afterburner configuration was permitted.

Hot spots on outer shell. - Hot spots on the outer shell consisted of small localized regions of the outer shell that glowed with high intensity during afterburning. The hot spots, in general, appeared between the flame holder and the exhaust nozzle and resulted from direct impingement of combustion gases on the inside of the outer shell in the affected area. The hot spots were undesirable because of their random and unpredictable nature and because of the fact that some kind of external shell cooling system would, in all probability, have to be provided if the hot spots were permitted to exist. No local outer-shell surface temperature measurements were made, and as a result it cannot be stated definitely that these hot spots could not be tolerated in some specific cases.

Configurations employing all four of the innerbodies were subject to hot spots. Attempts to eliminate the hot spots included changes in the longitudinal fuel-injection stations, radial shifts of fuel-spray bars, and removal of specific fuel-injection spray bars upstream of the affected area. These fuel-injection-system changes did not eradicate the outer shell hot spots.

The only successful means of eliminating the outer-shell hot spots was found simultaneously with the remedy established for combustion screech. (Combustion screech is discussed in the following section.) The special equipment used in the elimination of outer-shell hot spots consisted of a perforated outer-shell liner (fig. 4). The liner provided for a positive flow of turbine-discharge gas between the liner and outer shell and thus isolated the outer shell from any irregularities in the combustion process. The relatively cool turbine-discharge gas between the liner and outer shell flowed into the combustion chamber through the perforations in the liner. The liner was similar in principle to the louvered liner reported in reference 3.

One perforated-liner afterburner (configuration 4B) was operated at an over-all engine-afterburner fuel-air ratio of 0.052 without appearance of hot spots on the outer shell or evidence of damage to the liner itself. The possibilities and limitations of the perforated-liner scheme were not fully explored, however. It is possible that the maximum potential afterburner output could not be realized with a perforated liner of the type investigated because of inability to burn fuel stoichiometrically in the cooling air.

Screeching combustion. - Screeching combustion (refs. 2, 4, and 5) was encountered on all short afterburner configurations that did not incorporate special means for its elimination. The audible frequency of screech varied from 780 cycles per second for configuration 6 to 1760 cycles per second for configuration 7. In general, screech occurred as fuel-air ratio was being increased; and below some limiting fuel-air ratio screech did not occur. For example, screech occurred above over-all engine-afterburner fuel-air ratios of 0.044 for configuration 6 and above 0.054 for configuration 7. For an ideal maximum-output engine-afterburner thermodynamic cycle, optimum operation would occur at an over-all stoichiometric fuel-air ratio (near 0.067); the limitations of screech on afterburner output are thus obvious if operation with screeching combustion must be avoided. Experience has indicated (ref. 6, e.g.) that screeching combustion in an afterburner should be avoided and can, at the pressure levels prevailing in the afterburner during sea-level static operation, be violently destructive of afterburner components if allowed to continue even for a fraction of a minute. Some minor failures due to screeching combustion were observed in the short afterburner configurations, but generally a run would be terminated if the audible manifestation of screech (in the control room) indicated that the screech was becoming intolerable.

A large number of theories were pursued and many techniques were employed in an effort to eliminate screech in the short afterburners. For example, on the basis of results obtained in reference 5, a water-cooled splitter plate was extended downstream of the apex of a single-ring flame holder (configuration 8). This configuration did not screech at over-all fuel-air ratios up to 0.060, where a configuration similar in all respects except for the splitter had screeched. The practical limitations imposed by requirements for cooling the splitter plate are obvious, however, and a more satisfactory solution to the problem of screeching combustion was sought.

A frequency of 1560 cycles per second, which was observed with many of the configurations, and equations describing the behavior of acoustic resonance suggested that screech was characterized by an acoustic resonance of the fourth lateral mode. Longitudinal acoustic fences (fig. 3) were used on the outer shell in configuration 7 in an attempt to dampen the oscillations predicted by this theory. The acoustic fences noticeably softened the audible manifestations of screech and increased the screech frequency from 1560 to 1760 cycles per second.

A perforated liner on the outer shell was tried in an attempt to absorb acoustic disturbances that might be associated with screech and that might, by reflecting from the outer shell, cause or support the screeching phenomenon. The perforated liner (fig. 4) was investigated

with the 24-inch innerbody in configuration 4B. A positive remedy for screech was observed with this configuration, inasmuch as no screech was obtained over the operable range of fuel-air ratios. Screech had been experienced with configuration 5, which was identical to configuration 4B in all respects except for the outer-shell liner, and with configuration 9, which had a single-ring 3/4-inch-gutter flame holder and no outer-shell liner. An indication of the screech-preventive qualities of the perforated liner was also obtained with configurations 10 and 11, which incorporated single-ring flame holders with gutter widths of 1.50 and 3 inches, respectively; these were investigated for screech because reference 5 had reported that screech tendency increases with increasing gutter width. No screech was observed with either configuration.

### Over-All Engine-Afterburner Performance

The performance of the engine and short afterburner combination was evaluated both with and without the afterburner in operation. Performance with the afterburner in operation is obviously important with respect to the available augmented thrust. Performance without the afterburner in operation is important from considerations of economic engine operation during cruise flight.

Afterburning. - In afterburner operation, flame seated on the downstream face of the innerbody and served to pilot the main combustion process. It was desirable, particularly for starting the afterburner, to interconnect the flame holder with this piloting zone through small radial elements on the flame holder (fig. 6). These interconnecting struts were not provided on flame holders used with the 24-inch innerbody, and starting was found to be more difficult than for configurations using other innerbodies. The fuel-air ratio in the piloting region on the downstream face of the innerbody was found to affect the combustion stability. Efforts were made in the design of the fuel-injection spray bars to provide a uniform fuel-air mixture across the annular passage of the diffuser, except near the outer wall. Moving the fuel-spray bars radially outward from their normal position (fig. 7), and thus tending to produce leaner mixtures in the piloting region on the downstream face of the innerbody, tended to promote rough combustion.

Afterburning data typical of those obtained with one of the fixed-area exhaust-nozzle configurations are plotted in figure 10. Turbine-outlet temperature, corrected thrust, and primary-engine fuel-air ratio are plotted as functions of over-all fuel-air ratio for an engine speed of 7900 rpm and an engine-inlet temperature of 100° F. The over-all fuel-air ratio is the sum of the primary-engine fuel-air ratio plus the

afterburner fuel-air ratio. Variations in over-all fuel-air ratio are due primarily to variations in the afterburner fuel-air ratio, as can be seen by the small variations in primary-engine fuel-air ratio in figure 10.

An increase in afterburner fuel-air ratio, hence in over-all fuel-air ratio, resulted in an increase in both turbine-outlet temperature and thrust (fig. 10). The over-all fuel-air ratio producing limiting turbine-outlet temperature would give the maximum thrust output for the particular exhaust-nozzle size used, and the thrust at this over-all fuel-air ratio represents the augmented engine performance that is consistent with safe engine operating limits. The definition of maximum engine output over a range of over-all fuel-air ratios would require data for a number of different exhaust-nozzle sizes at limiting turbine-outlet temperature (similar to fig. 10). Such data for different exhaust-nozzle sizes would represent the performance of the engine with a variable-area exhaust nozzle; a variable-area exhaust nozzle would be used in actual application so that maximum thrust output could be obtained both with afterburning at a preselected fuel-air ratio and without afterburning (shown by reference point in fig. 10). A series of fixed nozzles instead of a variable nozzle were used in the investigation reported herein in order to simplify the experimental apparatus.

An obvious property of the data shown in figure 10 is that changes in combustion efficiency will be reflected in the over-all fuel-air ratio required to give a specified turbine-outlet temperature. Although data similar to those shown in figure 10 were not recorded for all configurations, a knowledge of the relation between over-all fuel-air ratio and combustion efficiency was used to evaluate the effects of configuration changes on combustion efficiency. For example, it was found that increasing the number of gutter rings in the flame holder gave progressively higher combustion efficiency. The effects of the number of gutter rings were investigated by burning with flame seated on the innerbody alone and with flame holders having one and two annular rings. A two-ring flame holder with 0.75-inch gutters appeared to be generally satisfactory from the standpoint of combustion efficiency. It was also found that moving the fuel-spray bars upstream gave progressively improved combustion efficiency. Maximum combustion efficiency was obtained with the fuel-spray bars 5.25 inches downstream of the turbine discharge (station 5), which gave the maximum obtainable fuel-mixing distance for the short afterburner configurations. Farther upstream movement of the fuel-spray bars was prevented by the presence of the whirl-straightening vanes.

The performance of afterburner configurations 4, 4A, and 4B, which incorporated the 24-inch innerbody and the outer-shell liner, is shown in figure 11. These configurations were free of outer-shell hot spots and screech and are considered satisfactory for application in these

respects. Shown in figure 11 as functions of over-all fuel-air ratio are the afterburner-outlet temperature and the ratio of augmented afterburner thrust to the 5020-pound thrust of the standard nonafterburning engine under identical conditions of operation (7900 rpm and 1250° F tail-pipe temperature). Afterburning performance points are shown at only two over-all fuel-air ratios, since only two afterburning exhaust nozzles were available. These afterburning performance points were obtained at limiting turbine-outlet temperature.

Afterburner-outlet temperatures, which were calculated from measured thrust, air flow, and the ratio of total pressure in the plane of the exhaust-nozzle exit to the ambient exhaust pressure, are plotted in the upper part of figure 11, along with curves of constant combustion efficiency. Combustion efficiency is defined as the ratio of the temperature rise in the afterburner to the ideal temperature rise for the same increment of over-all fuel-air ratio used in the afterburner. Ideal afterburner-outlet temperatures for a combustion efficiency of 100 percent were obtained from reference 7. At an over-all fuel-air ratio of 0.042, the outlet temperature for the short afterburner was 2700° R and the combustion efficiency was 70 percent. At an over-all fuel-air ratio of 0.052, the afterburner-outlet temperature was 3350° R and the combustion efficiency was 85 percent.

A curve of afterburner-outlet temperature obtained with a long afterburner (ref. 6) is shown in figure 11 to indicate the performance losses that may be attributable to reduction in combustion-chamber length. The combustion-chamber length, including exhaust nozzle, for the afterburner used in the investigation of reference 6 was 57 inches compared with 36 inches for the short afterburner configurations reported herein. The combustion efficiency for the short afterburner was 30 percentage points lower than that for the long afterburner at a fuel-air ratio of 0.042, and 15 percentage points lower at a fuel-air ratio of 0.052.

In the lower portion of figure 11, a curve of augmented thrust ratio obtainable with a combustion efficiency of 100 percent is shown for reference purposes. The augmented thrust ratio of 0.97 obtained with the afterburner inoperative (over-all fuel-air ratio of 0.017) results from pressure losses in the short afterburner. At an over-all fuel-air ratio of 0.042, an augmented thrust ratio of 1.21 was obtained, compared with an ideally obtainable value of 1.31; at an over-all fuel-air ratio of 0.052, an augmented thrust ratio of 1.33 was obtained, compared with an ideally obtainable value of 1.42. Differences between the actual and ideal thrust ratios are caused by inefficiencies in combustion, as discussed previously. Improvements in combustion efficiency would improve fuel economy for any given thrust augmentation and would make more nearly realizable the maximum potential output for the afterburner (an augmentation ratio of 1.54 as indicated by the ideal curve).

The highest augmentation ratio obtained with the short afterburner (1.33) is not the established maximum for the particular configurations investigated. The maximum augmentation for the short afterburner configurations could not be determined with the limited number of exhaust-nozzle sizes available.

Some other short afterburner configurations investigated were not wholly acceptable because of outer-shell hot spots and combustion screech. Afterburning performance data were obtained on some of these configurations, however, and are shown in figure 12, where afterburner-outlet temperature and augmented thrust ratio are plotted against overall fuel-air ratio. A comparison of the performance of the configurations shown in figure 12 with configurations 4A and 4B (fig. 11) reveals that, in general, the combustion efficiency was not radically altered by the design of the innerbody or the presence of the outer-shell liner. The poor performance of configuration 12 relative to the other configurations investigated is attributable to the downstream location of the fuel-injection system (just ahead of the flame holder) and the fact that the flame holder had only one annular ring.

Nonafterburning. - Although actual engine cruising conditions were not simulated in the short afterburner investigation, the normal non-afterburning performance obtained gives a good approximation of losses in performance at other operating conditions. As shown in figure 11, the thrust with no afterburning is 97 percent of the thrust of the standard nonafterburning engine at identical conditions of engine speed and tail-pipe temperature and, thus, fuel flow. A 3-percent penalty in specific fuel consumption due to pressure losses is thus chargeable to the short afterburner components. In application of the short afterburner to aircraft designed for long-range flight, this 3-percent increase in specific fuel consumption would have to be evaluated in terms of savings in weight of alternate assisted-take-off schemes that the short afterburner would replace and in terms of general operating convenience offered by the short afterburner.

As shown in reference 1, a short afterburner diffuser configuration without a flame holder, an outer-shell liner, or fuel spray bars gave an exhaust-nozzle-inlet pressure (hence thrust) only 1 percent lower than the standard engine gave. Possibilities for improving the nonafterburning performance of the short afterburner are thus indicated. The means of effecting improvements in the nonafterburning performance include optimization of flow through the perforated liner and either decreasing the flame-holder blockage without compromising afterburning performance or providing a means of retracting the flame holder when not in use.

## CONCLUDING REMARKS

3174 An investigation was conducted to determine some principles of design for and performance of a short afterburner which, with the compressor and turbine sections of the primary engine, would fit within an envelope of approximately the same size as a standard nonafterburning model of the turbojet engine. In this short afterburner, high diffusion rates were required so that space would be available for satisfactory combustion. Development of a satisfactory configuration was hampered by local hot spots on the shell of the afterburner and by screeching combustion, both of which were characteristic tendencies exhibited by all configurations investigated except those including a special afterburner-shell inner liner extending from the flame holder to the exhaust nozzle. This liner, by providing a blanket of cool unburned gas against the burner shell that flowed through perforations into the burner proper, eliminated the hot spots on the wall. The perforations in the liner damped the pressure oscillations associated with screeching combustion and eliminated all audible evidences of the phenomenon.

Flame-holder design and fuel-mixing distance were found to have important effects on the performance of the short afterburner, even at the high pressures associated with sea-level static operation. The short combustion chamber (36 in.) required that the fuel and air be well mixed for good combustion efficiency; best combustion efficiencies were obtained with the fuel-spray bars located as close to the turbine discharge as possible. A flame holder with two 0.75-inch annular rings gave better combustion efficiency than a flame holder with one ring. With the maximum available fuel-mixing distance and a two-ring flame holder, the combustion efficiency obtained with the short afterburner was still from 15 to 30 percentage points lower than for a long (57 in.) combustion chamber under similar operating conditions.

One short afterburner configuration that appeared to be satisfactory for application gave an augmented thrust 1.33 times the thrust of the standard nonafterburning engine model. The augmentation ratio of 1.33 was obtained at an over-all engine-afterburner fuel-air ratio of 0.052 with the largest of the fixed-exhaust-nozzle sizes available and does not represent the maximum output for the afterburner. Higher augmentation probably could have been obtained with larger exhaust-nozzle sizes and higher over-all fuel-air ratios. For the configuration that gave an augmentation ratio of 1.33, the nonafterburning specific fuel consumption was 3 percent higher than for the standard nonafterburning model of the engine.

Lewis Flight Propulsion Laboratory  
National Advisory Committee for Aeronautics  
Cleveland, Ohio, February 24, 1954

## REFERENCES

1. Mallett, William E., and Harp, James L., Jr.: Performance Characteristics of Several Short Annular Diffusers for Turbojet Engine Afterburners. NACA RM E54B09, 1954
2. Harp, James L., Jr., Velie, Wallace W., and Bryant, Lively: Investigation of Combustion Screech and a Method of its Control. NACA RM E53L24b, 1954.
3. Renas, Paul E., and Jansen, Emmert T.: Effect of Flame-Holder Design on Altitude Performance of Louvered-Liner Afterburner. NACA RM E53H15, 1953.
4. Bragdon, Thomas A., Lewis, George D., and King, Charles H.: Interim Report on Experimental Investigation of High Frequency Oscillations in Ram-Jet Combustion Chambers. M.I.T. Meteor Rep. UAC-53, Res. Dept., United Aircraft Corp., Oct. 1951. (BuOrd Contract NOrd 9845.)
5. Usow, Karl H., Meyer, Carl L., and Schulze, Frederick W.: An Experimental Investigation of Screeching Combustion in Full-Scale Afterburner. NACA RM E53I01, 1953.
6. Useller, James W., and Povolny, John H.: Experimental Investigation of Turbojet-Engine Thrust Augmentation by Combined Compressor Coolant Injection and Tail-Pipe Burning. NACA RM E51H16, 1951.
7. Mulready, Richard C.: The Ideal Temperature Rise Due to the Constant Pressure Combustion of Hydrocarbon Fuels. M.I.T. Meteor Rep. UAC-9, Res. Dept., United Aircraft Corp., July 1947. (BuOrd Contract NOrd 9845.)

3174

TABLE I. - AFTERBURNER CONFIGURATIONS

Config- uration	Innerbody	Outer shell	Fuel- injection station	Flame holder	Exhaust- nozzle diameter, in.
1	Modified curved	Basic	5	2-ring, 0.75-in.	a
2 2A 2B }	18-in. straight	Basic	5	2-ring, 0.75-in.	$\left\{ \begin{array}{l} a \\ 24.25 \\ 25.50 \end{array} \right.$
3 3A 3B }	18-in. slotted	Basic	6	2-ring, 0.75-in.	$\left\{ \begin{array}{l} a \\ 24.25 \\ 25.50 \end{array} \right.$
4 4A 4B }	24-in.	Liner	5	2-ring, 0.75-in.	$\left\{ \begin{array}{l} a \\ 24.25 \\ 25.50 \end{array} \right.$
5	24-in.	Basic	5	2-ring, 0.75-in.	25.50
6	Modified curved	Basic	7	1-ring, 0.75-in.	24.25
7	18-in. slotted	Longitudinal fins	6	2-ring, 0.75-in.	25.50
8	24-in.	Basic	5	1-ring, 3-in. with splitter	25.50
9	24-in.	Basic	5	1-ring, 0.75-in.	25.50
10	24-in.	Liner	5	1-ring, 1.50-in.	25.50
11	24-in.	Liner	5	1-ring, 3-in.	25.50
12	Modified curved	Basic	7	1-ring, 0.75-in.	24.25

<sup>a</sup>Approximately 20.5 inches. Sized to give limiting turbine-outlet temperature of 1250° F at 7900 rpm, no afterburning.

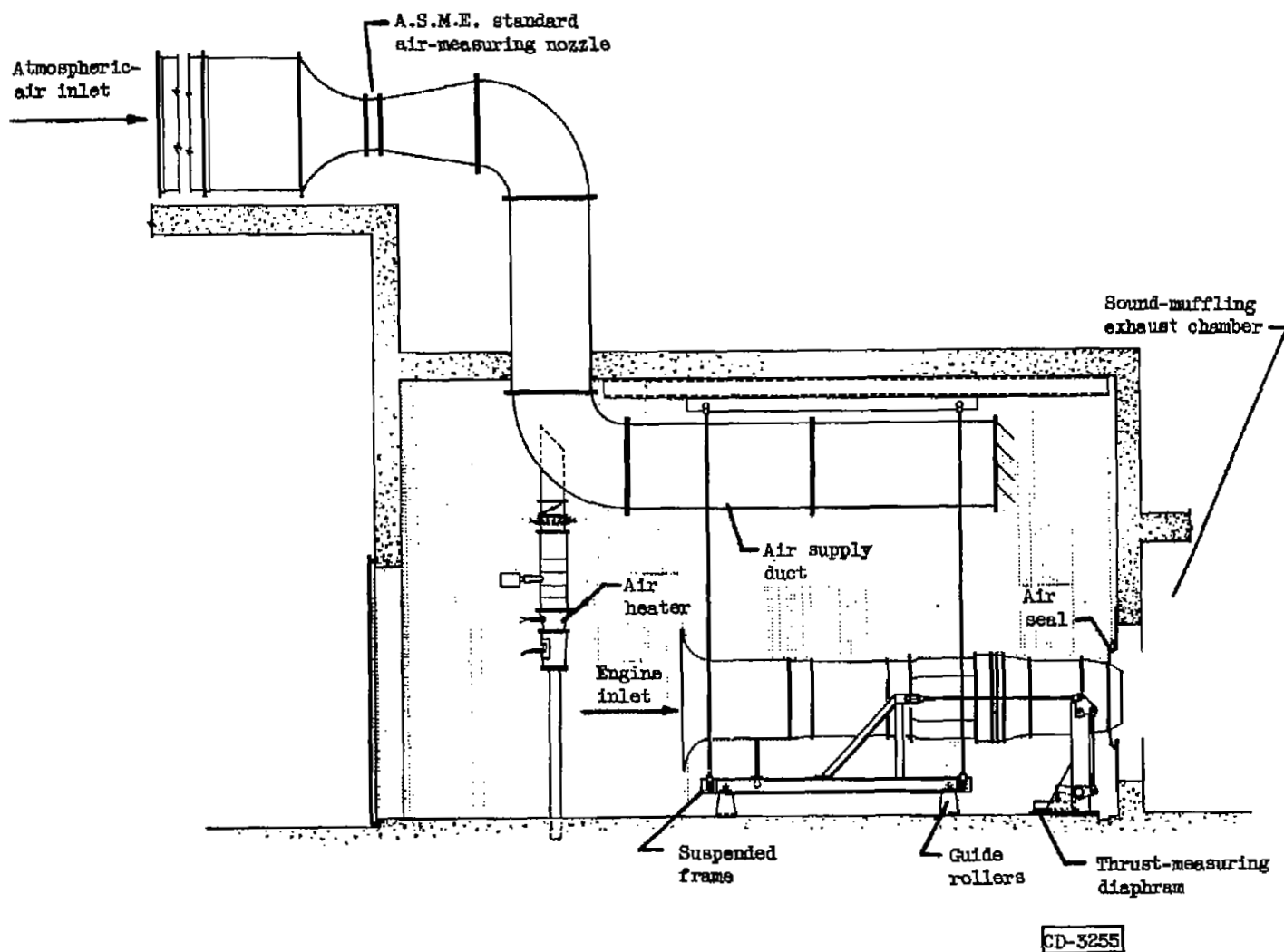


Figure 1. - Engine installation in test cell.

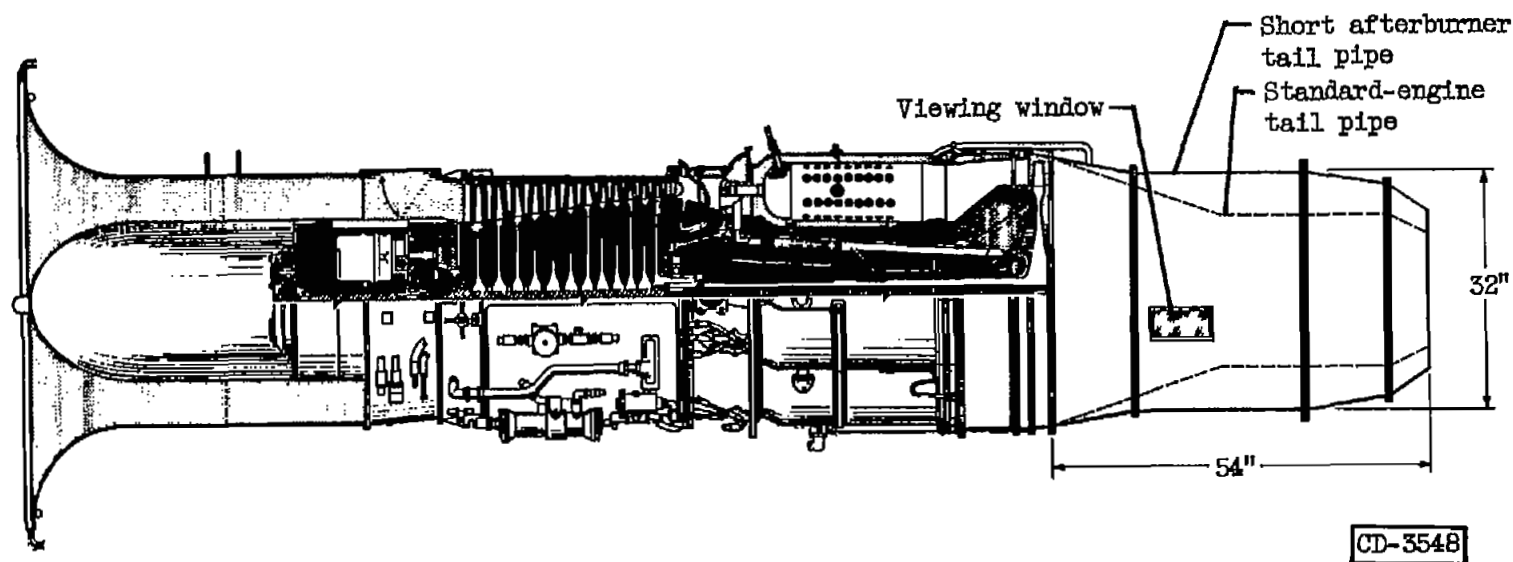
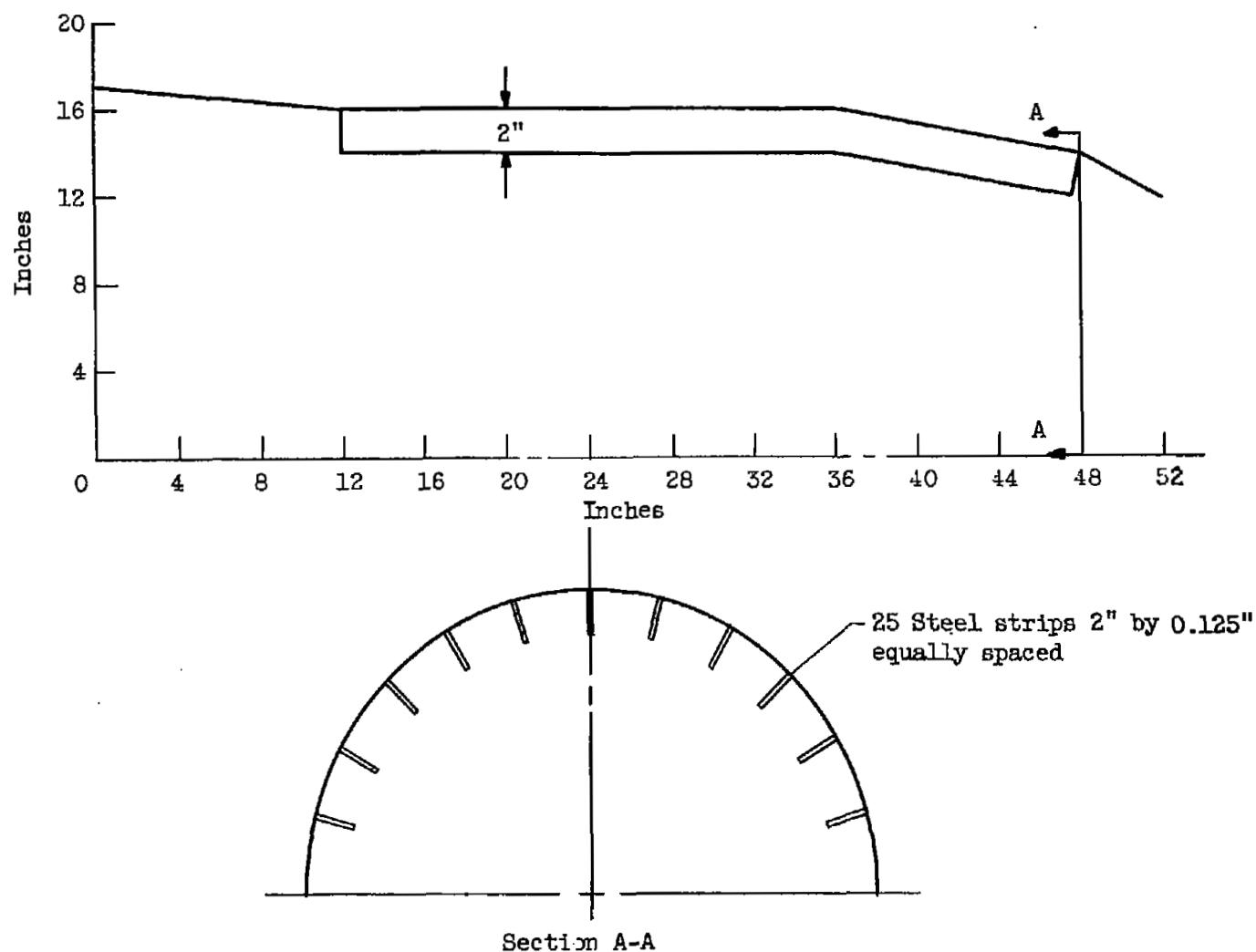
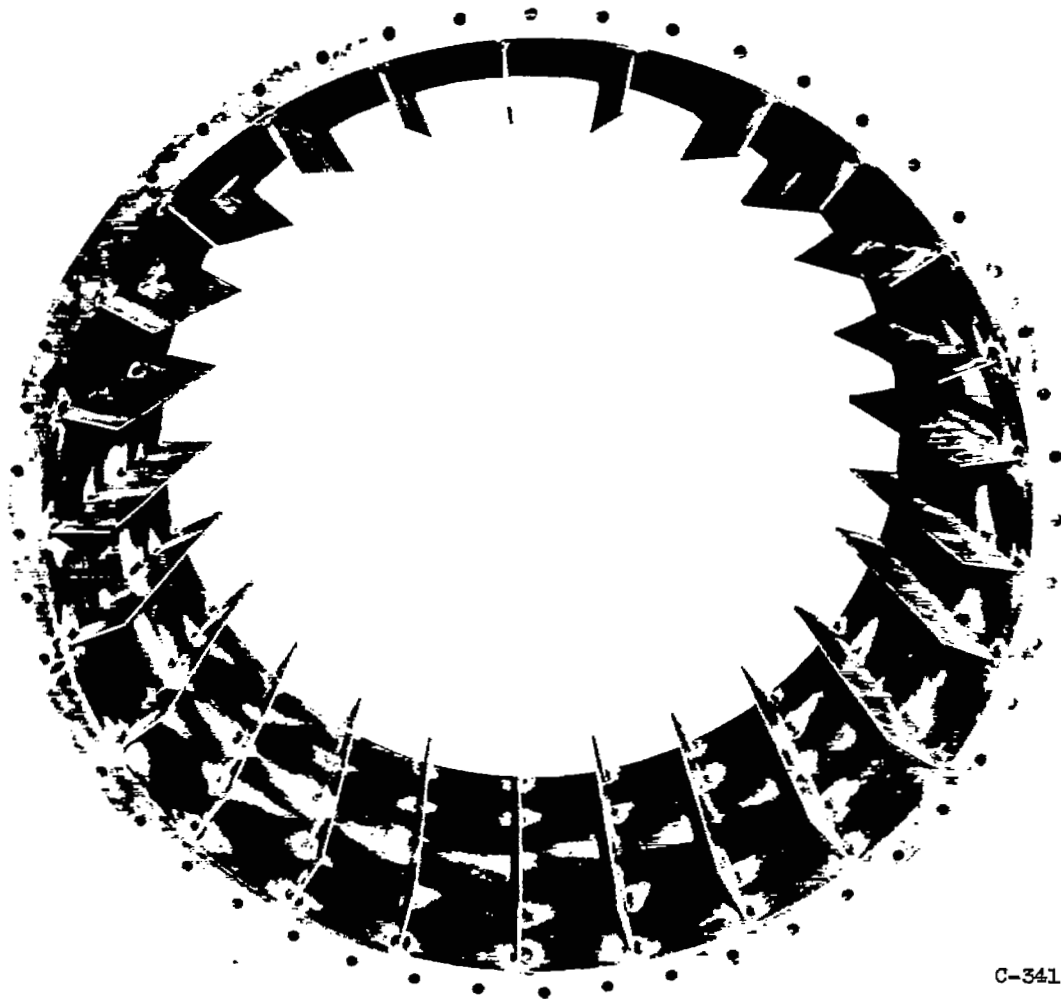


Figure 2 - Over-all engine envelopes of afterburning and standard nonafterburning engines.



Section A-A  
(a) Sketch of longitudinal fins.

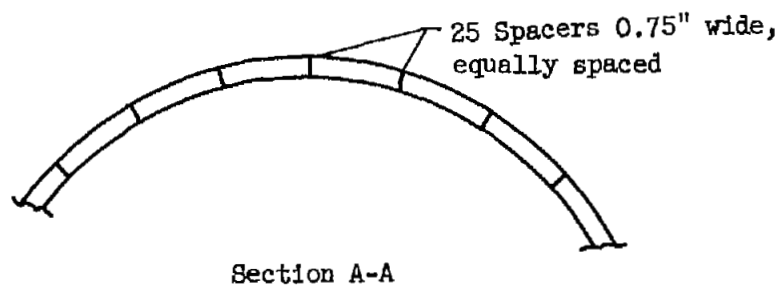
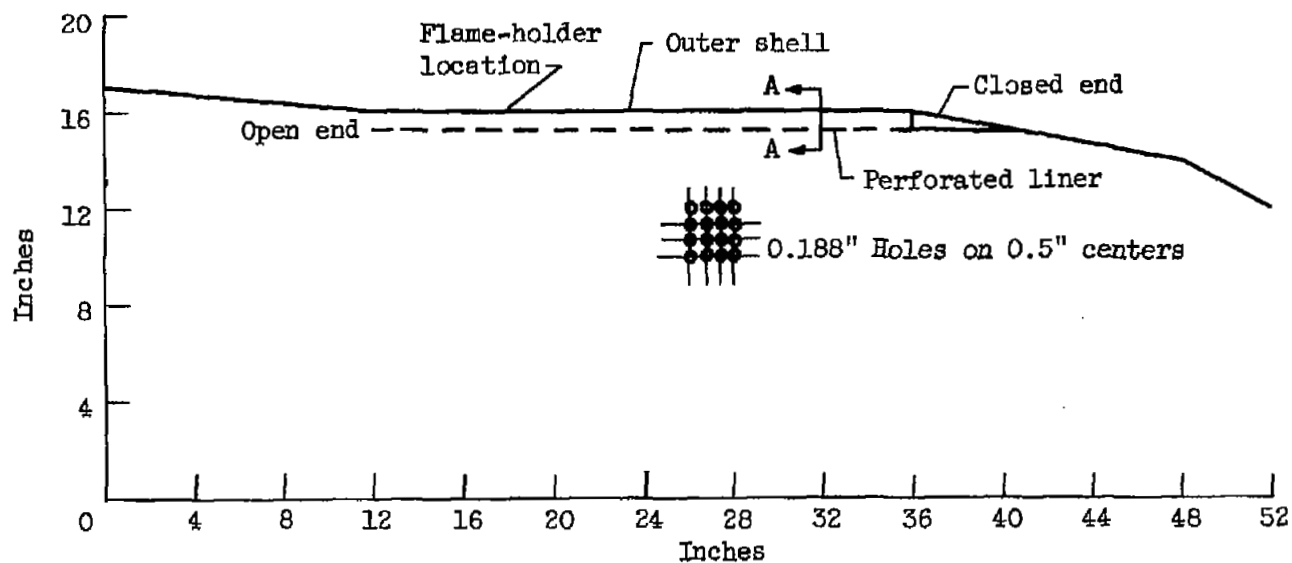
Figure 3. - Details of outer-shell longitudinal fins.



C-34198

(b) Photograph of longitudinal fins welded to inside of afterburner shell.

Figure 3. - Concluded. Details of outer-shell longitudinal fins.



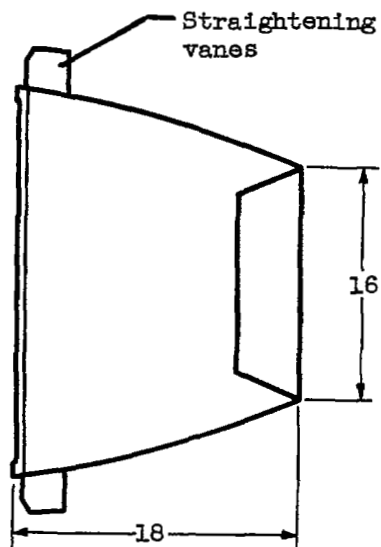
(a) Sketch of perforated liner.

Figure 4. - Details of outer-shell perforated liner.

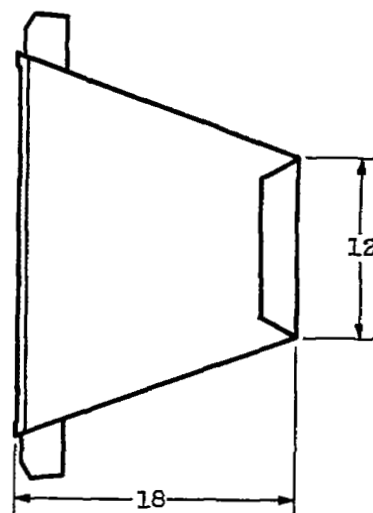


(b) Photograph of perforated liner installed in afterburner shell.

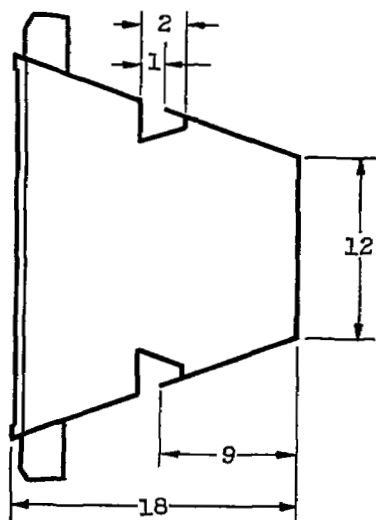
Figure 4. - Concluded. Details of outer-shell perforated liner.



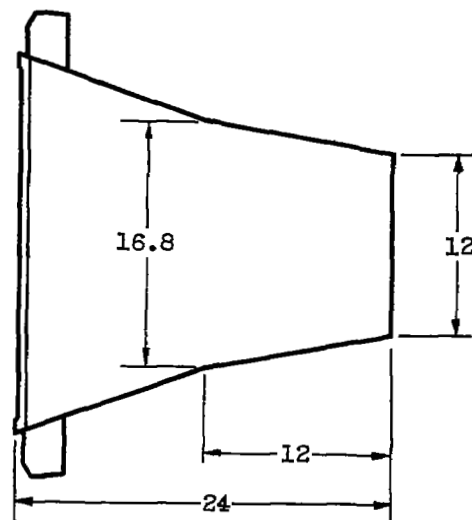
Modified curved



18-Inch straight



18-Inch slotted



24-Inch

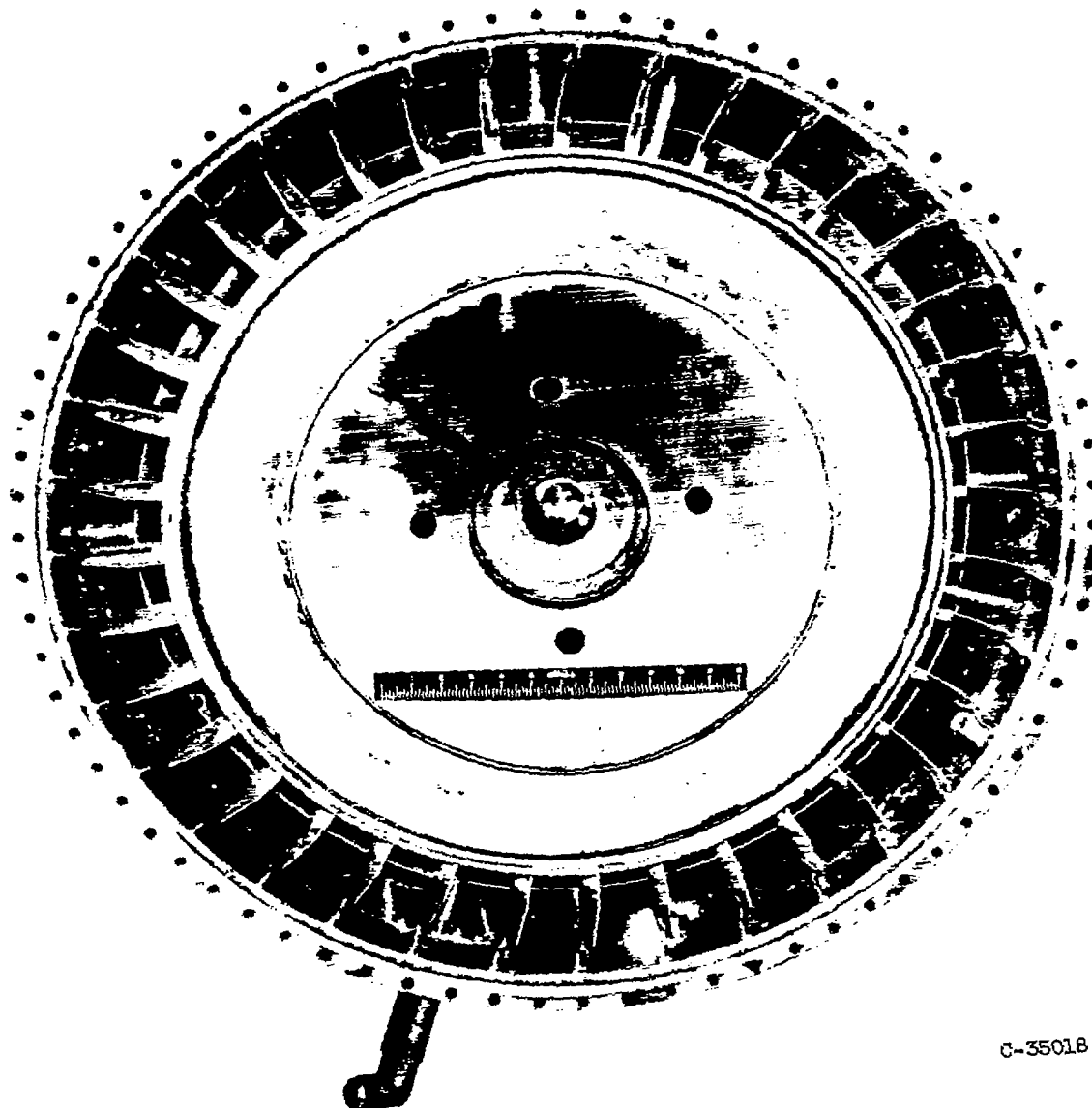
CD-3534

(a) Contours and dimensions (inches).

Figure 5. - Innerbodies investigated in short afterburner.

3174

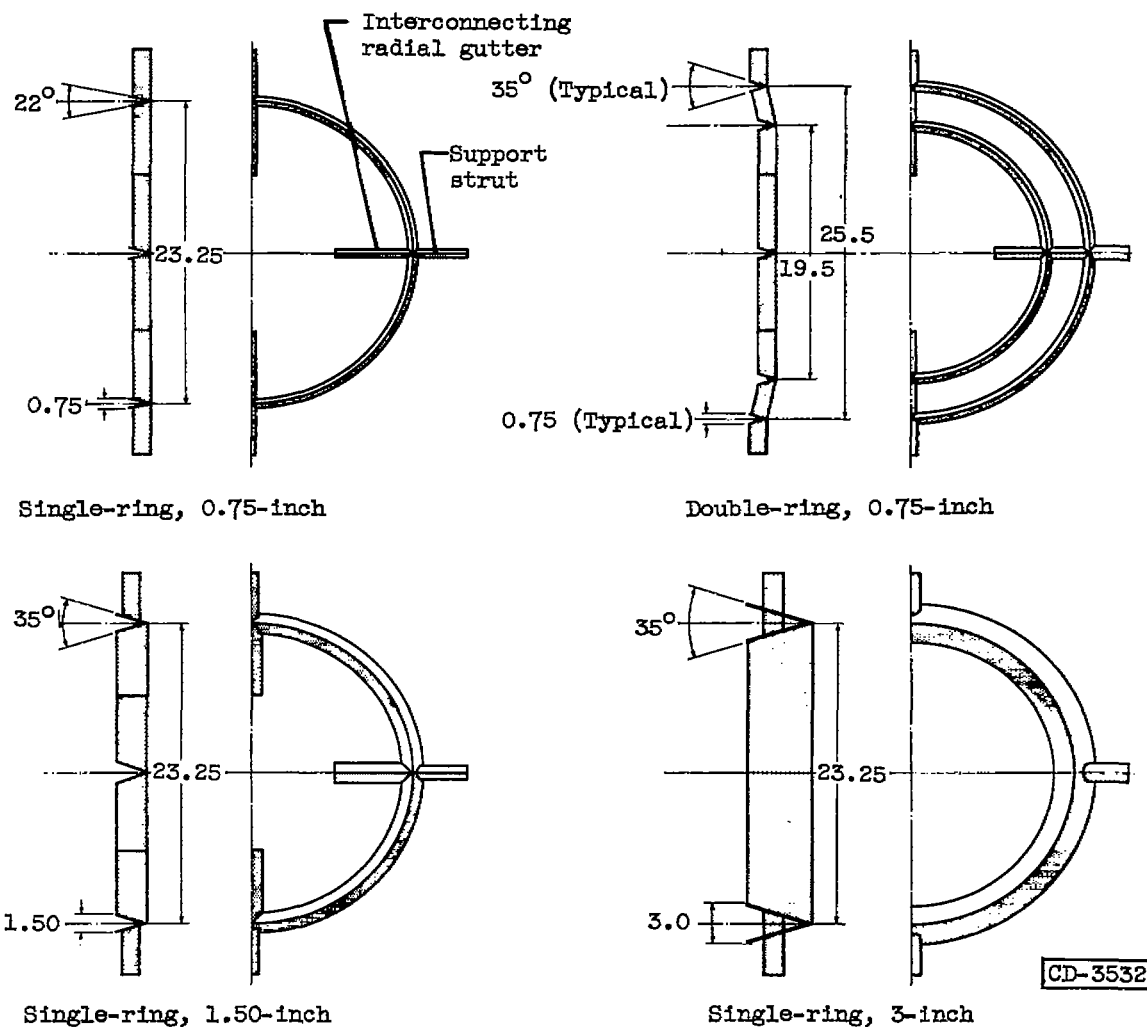
Civ-4



C-35018

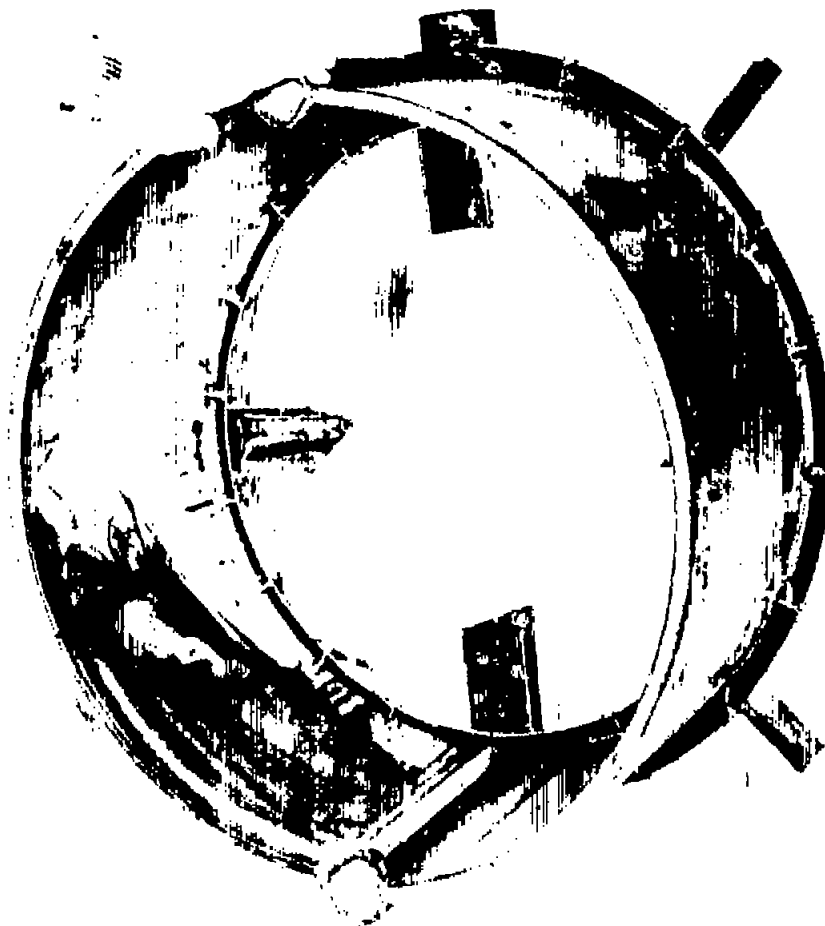
(b) Straightening vanes.

Figure 5. - Concluded. Innerbodies investigated in short afterburner.



(a) Sketches showing dimensions. (All dimensions in inches.)

Figure 6. - Flame holders used in investigation.



C-32617

(b) Single-ring 3-inch flame holder with water-cooled splitter added.

Figure 8. - Concluded. Flame holders used in investigation.

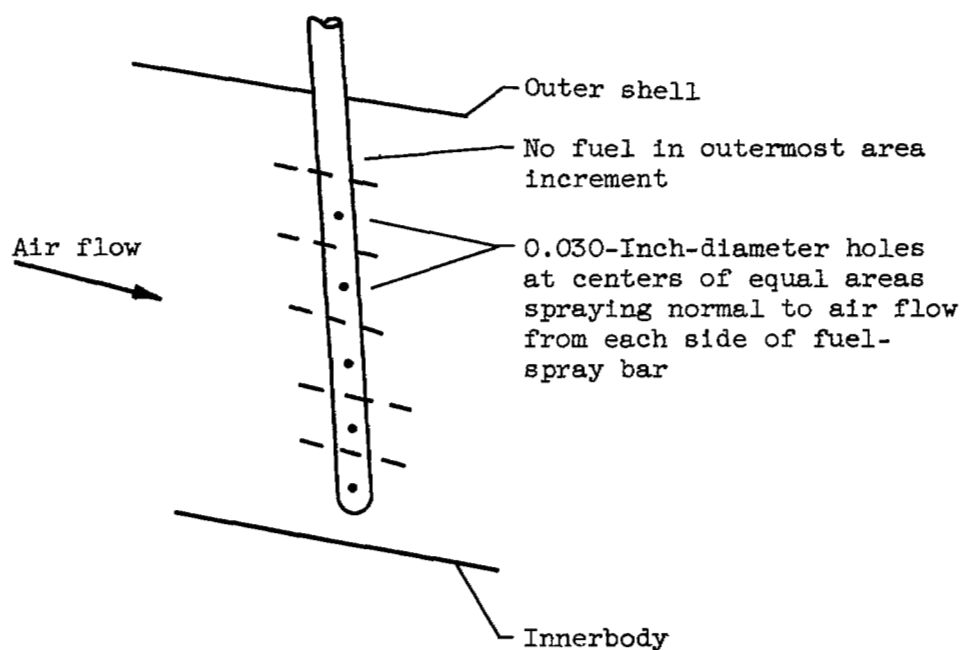


Figure 7. - Typical fuel-spray-bar construction.

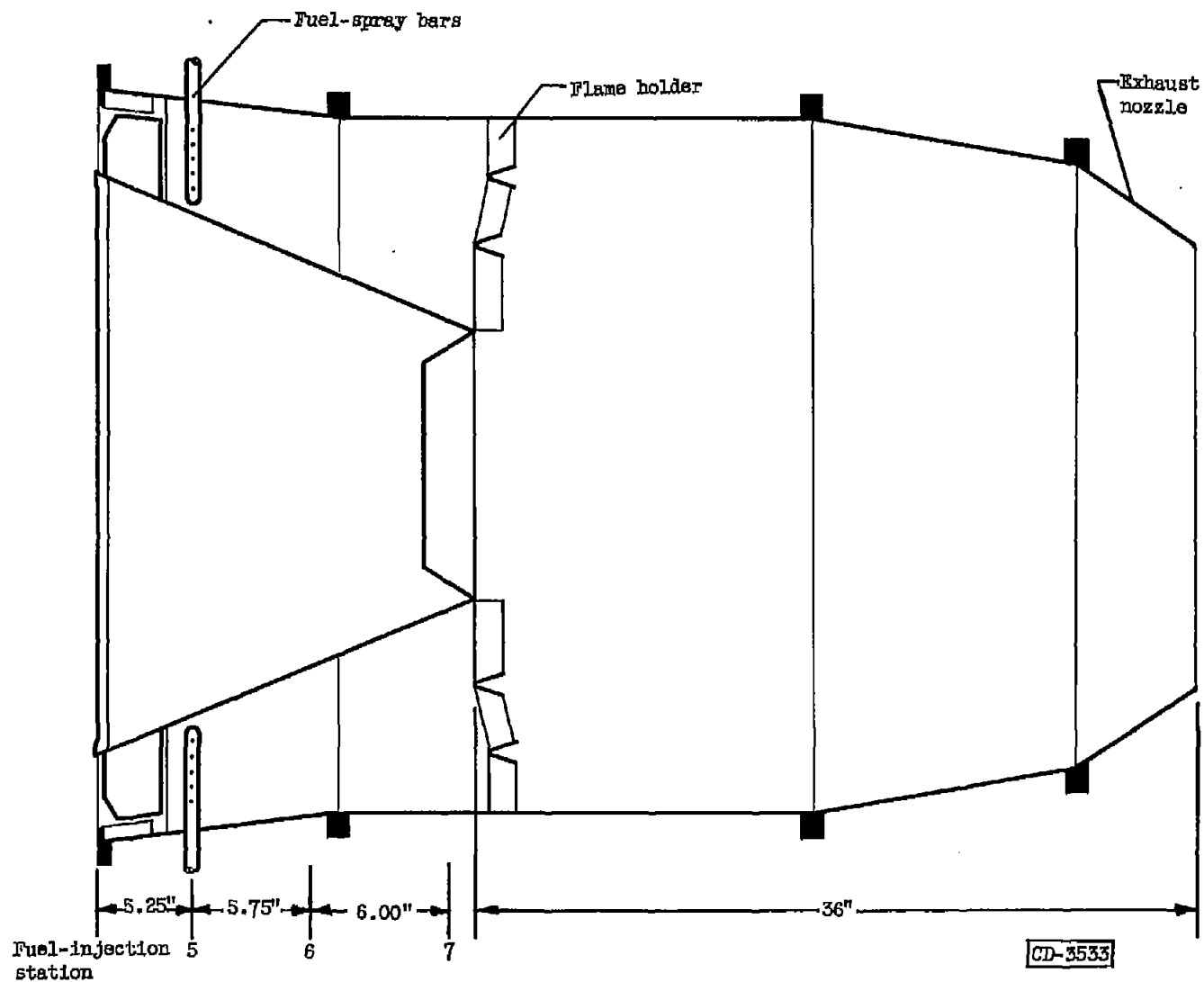


Figure 8. - Schematic diagram of typical short afterburner configuration (configuration 2).

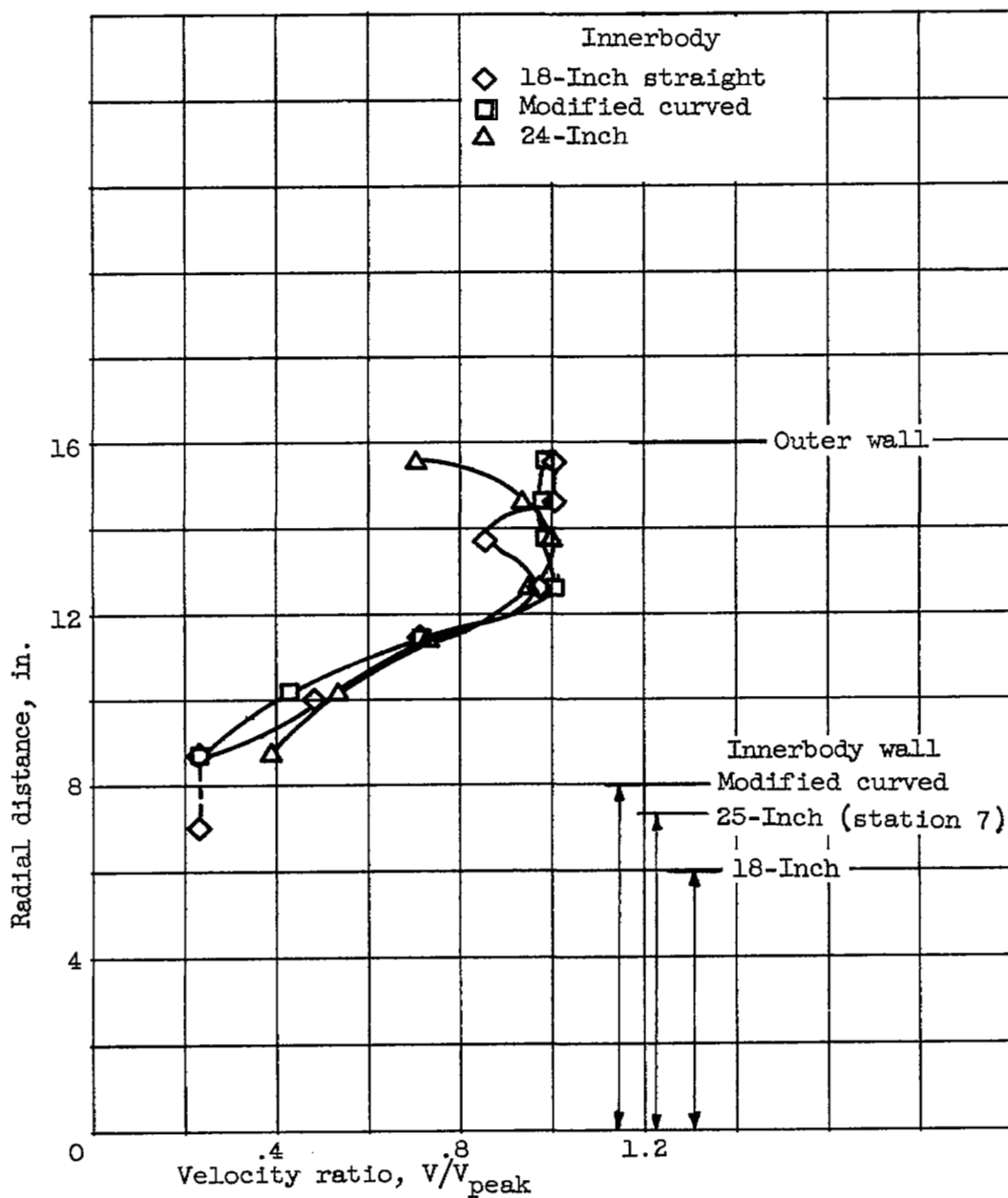


Figure 9. - Diffuser-outlet velocity profiles at station 7.  
 Engine speed, 7900 rpm; tail-pipe temperature, 1250° F;  
 no flame holder.

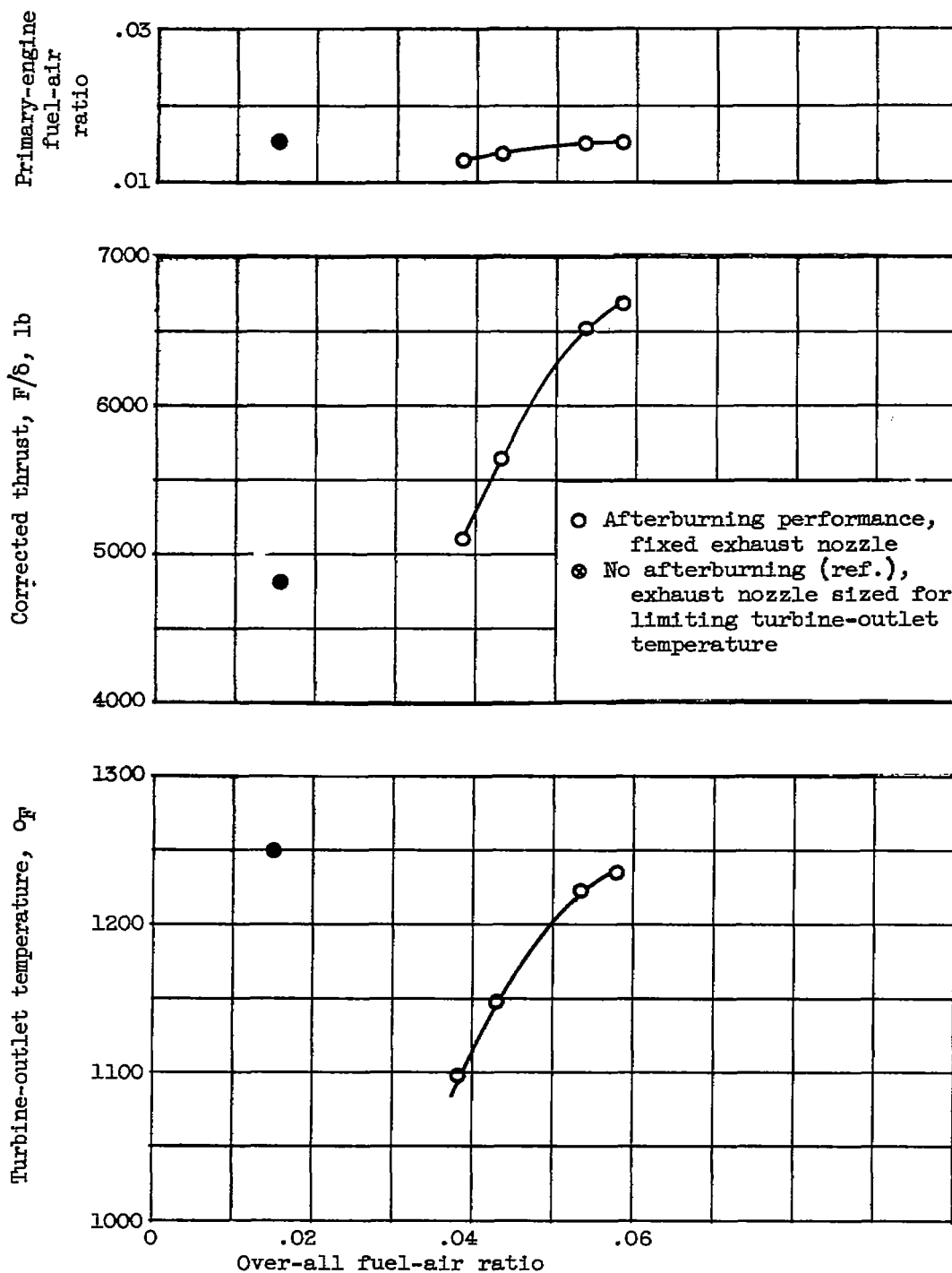


Figure 10. - Typical fixed-exhaust-nozzle afterburning data at engine speed of 7900 rpm and engine-inlet temperature of 100° F. Configuration 3B.

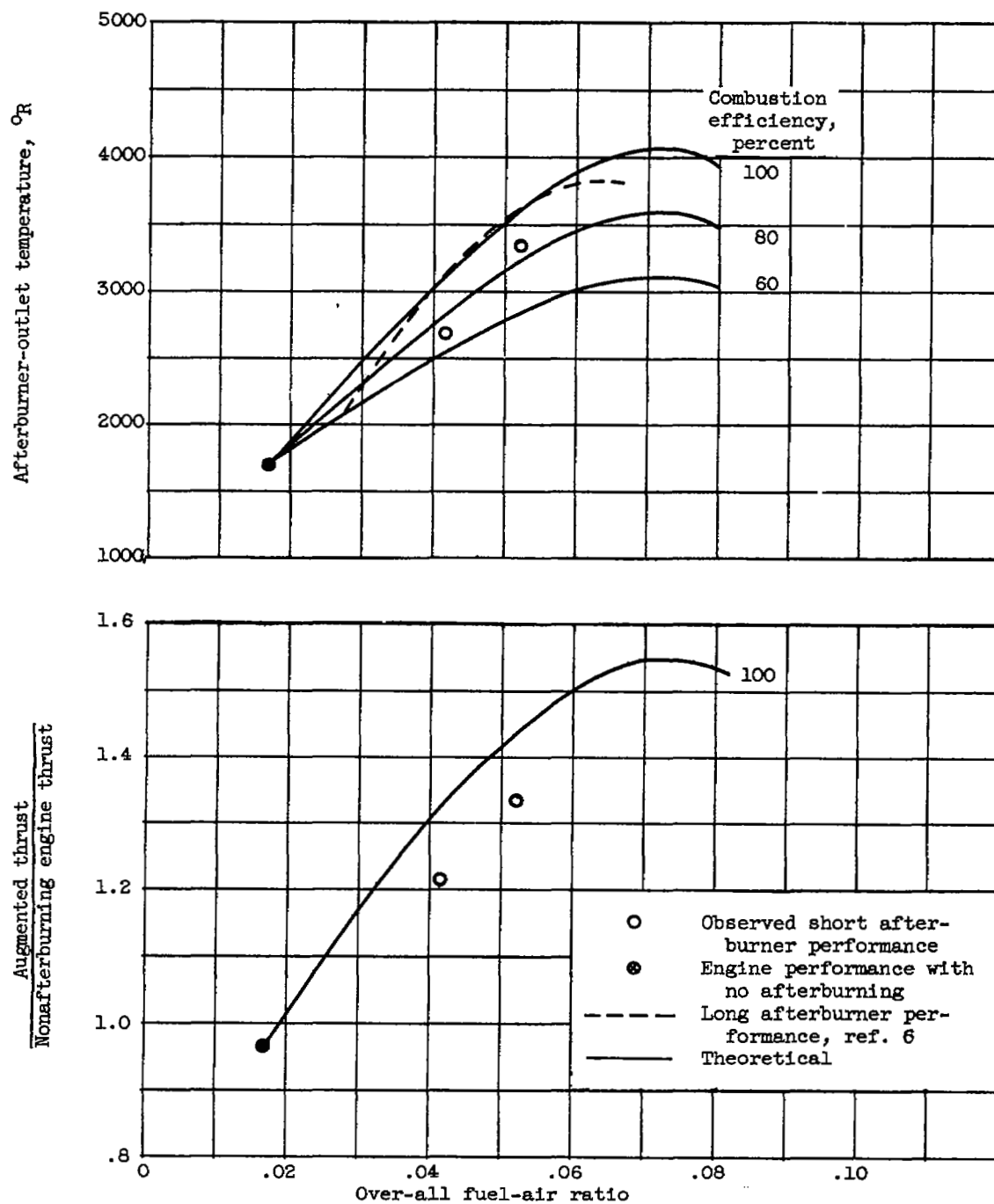


Figure 11. - Afterburning performance of 24-inch innerbody configurations (4, 4A, and 4B). Engine speed, 7900 rpm; engine-inlet temperature,  $100^{\circ}\text{F}$ ; turbine-outlet temperature,  $1250^{\circ}\text{F}$ .

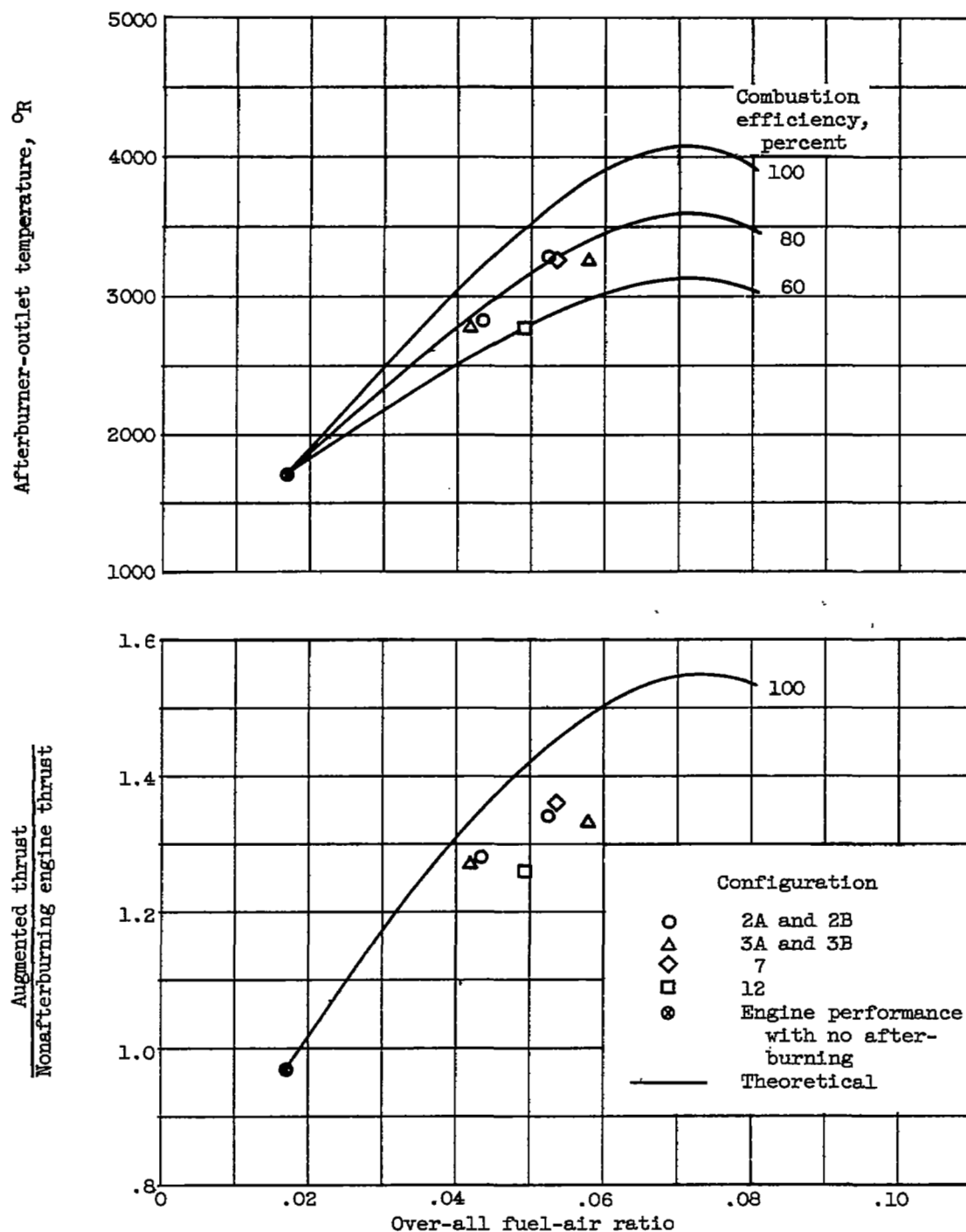


Figure 12. - Afterburning performance of various configurations.  
Engine speed, 7900 rpm; engine-inlet temperature, 100° F;  
turbine-outlet temperature, approximately 1250° F.

NASA Technical Library



3 1176 01435 3800

